

# Binary-liquid phase separation of lens protein solutions

( $\gamma$ -crystallin/coexistence curve/critical phenomena/cold cataract/homology)

MICHAEL L. BROIDE, CAROLYN R. BERLAND, JAYANTI PANDE, OLUTAYO O. OGUN,  
AND GEORGE B. BENEDEK\*

Department of Physics and Center for Materials Science and Engineering, Massachusetts Institute of Technology, Cambridge, MA 02139

Contributed by George B. Benedek, April 1, 1991

**ABSTRACT** We have determined the coexistence curves (plots of phase-separation temperature  $T$  versus protein concentration  $C$ ) for aqueous solutions of purified calf lens proteins. The proteins studied, calf  $\gamma$ IIIa-,  $\gamma$ IIIb-, and  $\gamma$ IVa-crystallin, have very similar amino acid sequences and three-dimensional structures. Both ascending and descending limbs of the coexistence curves were measured. We find that the coexistence curves for each of these proteins and for  $\gamma$ II-crystallin can be fit, near the critical point, to the function  $|(C_c - C)/C_c| = A[(T_c - T)/T_c]^\beta$ , where  $\beta = 0.325$ ,  $C_c$  is the critical protein concentration in mg/ml,  $T_c$  is the critical temperature for phase separation in K, and  $A$  is a parameter that characterizes the width of the coexistence curve. We find that  $A$  and  $C_c$  are approximately the same for all four coexistence curves ( $A = 2.6 \pm 0.1$ ,  $C_c = 289 \pm 20$  mg/ml), but that  $T_c$  is not the same. For  $\gamma$ II- and  $\gamma$ IIIb-crystallin,  $T_c \approx 5^\circ\text{C}$ , whereas for  $\gamma$ IIIa- and  $\gamma$ IVa-crystallin,  $T_c \approx 38^\circ\text{C}$ . By comparing the published protein sequences for calf, rat, and human  $\gamma$ -crystallins, we postulate that a few key amino acid residues account for the division of  $\gamma$ -crystallins into low- $T_c$  and high- $T_c$  groups.

The  $\gamma$ -crystallins constitute a family of highly homologous mammalian lens proteins (1–4). Concentrated aqueous solutions of  $\gamma$ -crystallins (5–8) exhibit the phenomena of binary-liquid-phase separation (9–11), also known as coacervation (12). These solutions separate into two coexisting liquid phases of unequal protein concentration at temperatures less than the critical temperature for phase separation  $T_c$ . From previous studies (5, 7, 8), it is known that location of the coexistence curve depends sensitively on the amino acid sequence of the crystallin molecule. Two distinct groups of  $\gamma$ -crystallins have been identified in rat (7) and human (8) lenses: high- $T_c$  crystallins and low- $T_c$  crystallins. In these rat and human studies, the precise values of  $T_c$  for each crystallin, though inferred from the data, were not determined explicitly. For the high- $T_c$  crystallins, only the ascending limb of the coexistence curves was measured. For the low- $T_c$  crystallins, only an upper bound for the  $T_c$  values was established.

In this paper, we report on measurements of coexistence curves for three purified calf  $\gamma$ -crystallins— $\gamma$ IIIa,  $\gamma$ IIIb, and  $\gamma$ IVa—in Table 2 we indicate the current nomenclature for mammalian  $\gamma$ -crystallins (2)] and for the native calf  $\gamma$ -crystallin mixture  $\gamma$ IV. We have determined both the ascending and descending limbs of each coexistence curve. This information enables us to characterize the coexistence curves in detail and to determine explicitly the values of the critical concentration  $C_c$  and the critical temperature  $T_c$  for each protein. Such detailed analysis of  $\gamma$ -crystallin phase separation, which requires gram quantities of purified protein, has been performed only for calf  $\gamma$ II (6).

We find that the purified calf  $\gamma$ -crystallins, in accord with the purified rat and human  $\gamma$ -crystallins, fall into two distinct groups: high- $T_c$  ( $T_c > 35^\circ\text{C}$ ) proteins,  $\gamma$ IIIa and  $\gamma$ IVa, and low- $T_c$  ( $T_c < 10^\circ\text{C}$ ) proteins,  $\gamma$ II and  $\gamma$ IIIb.

Because the  $\gamma$ -crystallins are highly homologous proteins, we are able to relate the observed differences in their  $T_c$  values to specific differences in their amino acid sequences. We have compared the published sequences of the calf, rat, and human  $\gamma$ -crystallins and find that a few key residues may account for division of the proteins into high- and low- $T_c$  groups. This correlation between molecular features and phase behavior provides an important step in identifying the physical and chemical factors that set the value of  $T_c$ . Because protein phase separation is one of the mechanisms for lens opacification (13–16), a quantitative understanding of the phase behavior of  $\gamma$ -crystallin solutions may suggest ways to treat and prevent certain types of cataracts.

## MATERIALS AND METHODS

**Protein Isolation and Purification.** The  $\gamma$ -crystallins used in this study were isolated from 1- to 6-week-old calf lenses, obtained by overnight express from Antech (Tyler, TX). The monomeric  $\gamma$ -crystallins were prepared from the soluble protein fraction by size-exclusion chromatography on Sephadex G-75, as described earlier (6). Native  $\gamma$ -crystallin so obtained was further fractionated into  $\gamma$ I,  $\gamma$ s,  $\gamma$ II,  $\gamma$ III, and  $\gamma$ IV, by cation-exchange chromatography on sulfopropyl Sephadex C-50, essentially according to Björk (17) and Thomson *et al.* (6).

Anion-exchange chromatography on DEAE-Sephadex was used to fractionate  $\gamma$ III into  $\gamma$ IIIa and  $\gamma$ IIIb. A variation of the procedures described by Slingsby and Miller (18) and Thomson *et al.* (6) was used. Solutions of  $\gamma$ III were dialyzed exhaustively into 25 mM ethanolamine buffer, pH 8.8. The dialyzed solution of  $\gamma$ III, containing 800–900 mg of protein, was loaded onto a  $2.5 \times 40$  cm DEAE-Sephadex A-25 column equilibrated with the same buffer and eluted with a linear NaCl gradient increasing from 0 to 100 mM.  $\gamma$ IIIb eluted first, followed by  $\gamma$ IIIa. Native  $\gamma$ III consists of (by fraction number)  $\approx 60\%$   $\gamma$ IIIb and  $\approx 40\%$   $\gamma$ IIIa. Immediately after elution, the two proteins were transferred into 275 mM sodium acetate buffer, pH 4.8, to prevent possible oxidation of sulphydryl groups.

$\gamma$ IV obtained by cation-exchange chromatography was further purified into  $\gamma$ IVa, the major fraction (80–85%, by fraction number), and  $\gamma$ IVb, the minor fraction (10–15%), by the method of Pande and Chakrabarti (A. Pande, personal communication). These results are comparable to those obtained by HPLC (19) and chromatofocusing (18).

The publication costs of this article were defrayed in part by page charge payment. This article must therefore be hereby marked "advertisement" in accordance with 18 U.S.C. §1734 solely to indicate this fact.

Abbreviations:  $T_c$ , critical temperature for phase separation;  $C_c$ , concentration of protein in mg/ml;  $C_c$ , critical protein concentration; low- $T_c$  means  $T_c < 10^\circ\text{C}$ ; high- $T_c$  means  $T_c > 35^\circ\text{C}$ .

\*To whom reprint requests should be addressed.

The purified crystallin fractions were dialyzed exhaustively into 100 mM sodium phosphate buffer (ionic strength 240 mM, pH 7.1), which contained sodium azide (3 mM). These dialyzed solutions were then concentrated as described below. The purity of the  $\gamma$ IIIa,  $\gamma$ IIIb, and  $\gamma$ IVa fractions was at least 95%, based on chromatography and isoelectric focusing. All coexistence curves were determined from freshly purified fractions.

**Concentrating the Proteins.** We concentrated the protein solutions by using two techniques. The first technique, ultrafiltration (Amicon Centricon-10 and Centriprep-10), was used to concentrate  $\gamma$ IIIb to  $\approx 250$  mg/ml,  $\gamma$ IIIa to  $\approx 200$  mg/ml, and  $\gamma$ IV and  $\gamma$ IVa to  $\approx 100$  mg/ml. Protein solutions were ultrafiltered and stored at a temperature above the phase-separation temperature. For the low- $T_c$  protein,  $\gamma$ IIIb, this temperature was 20°C, well above its  $T_c$ , and for the high- $T_c$  proteins,  $\gamma$ IIIa,  $\gamma$ IV, and  $\gamma$ IVa, this temperature was 40°C, only slightly above  $T_c$ , but well below the denaturation temperature for  $\gamma$ -crystallin, which we estimate to be 65–70°C. Above 65–70°C,  $\gamma$ -crystallin solutions became irreversibly turbid, due to the formation of insoluble protein aggregates.

The second technique used to concentrate the proteins was phase-separation itself. Samples concentrated to 100–250 mg/ml by ultrafiltration were placed in a thermostated bath set below  $T_c$ , and the protein-rich phase that subsequently formed was collected. This technique, which is a practical application of the phenomenon of phase separation, allowed us to generate samples with protein concentrations as high as 470 mg/ml.

We anticipate that the Donnan effect (20) is negligible for  $\gamma$ -crystallin solutions because the pH of the sodium phosphate buffer (7.1) is very near the isoelectric point for the proteins (7.4–7.9; ref. 21). We, therefore, do not expect that the procedures used to concentrate the proteins induce a change in the buffer concentration or the pH of the sample. The coexistence curves in Figs. 1 and 3 were obtained from multiple batches of protein, each batch being concentrated in a slightly different way. The self-consistency of the data from these different batches confirms that the solution conditions were, in fact, held constant because  $T_c$  depends sensitively on the buffer concentration and solution pH.

For all the calf  $\gamma$ -crystallin solutions we studied, for solutions of calf  $\gamma$ II (6), and for solutions of lysozyme (22–24), the coexistence curve lies below the solid-liquid phase boundary. This result implies that over the range of concentration and temperature for which binary-liquid phase separation occurs, the equilibrium state of the solution consists of a liquid phase coexisting with a crystalline phase. We have performed a systematic study of the location of the solid-liquid phase boundary, the so-called liquidus line, for calf  $\gamma$ II-,  $\gamma$ IIIa-,  $\gamma$ IIIb-, and  $\gamma$ IV-crystallin. The results of this study will be published separately.

In the current study, we required crystal-free solutions and employed several techniques to inhibit crystal formation (6). We filtered the dilute (1–10 mg/ml) protein solutions before concentrating them; we rinsed all glassware and apparatus with dust-free water or buffer; and we used gentle, non-stirred, ultrafiltration devices to concentrate the protein solutions. If, despite our precautions, a sample did develop protein crystals, we were able to dissolve the crystals by diluting the sample and heating it to 40°C. The low- $T_c$  protein crystals dissolved in solutions diluted to  $\approx 10$  mg/ml. The high- $T_c$  protein crystals were more difficult to dissolve due to the location of their liquidus lines; these samples had to be diluted to  $\approx 1$  mg/ml. Once crystal-free, diluted samples were filtered and then reconcentrated.

Protein concentrations were determined using UV absorption spectroscopy. A small aliquot (typically 5–10  $\mu$ l) of the protein sample under investigation was diluted by a known

proportion in 100 mM phosphate buffer, and the UV absorption of the resulting solution was measured. A positive-displacement pipette (Gilson Microman) was used to pipette highly concentrated (viscous) protein solutions. The specific absorbance coefficients  $E_{280}^{0.1\%,1\text{cm}}$  used in these studies were determined by Pande (A. Pande, personal communication) and are listed in Table 1.

**Determination of Coexistence Curves.** We determined the coexistence curves by using two previously described methods (6, 22): the cloud-point method and the temperature-quench method. In the cloud-point method, we determined the opacification temperature for a fixed protein concentration. In the temperature-quench method, we determined the protein concentrations of the two coexisting liquid phases for samples held at a fixed temperature below  $T_c$ . The results of these two methods generally agreed with one another. Far below the critical point, the cloud-point data was systematically higher in temperature than the temperature-quench data.

It was difficult to prepare crystal-free highly concentrated samples of the high- $T_c$  proteins. As a consequence, the coexistence curves for  $\gamma$ IIIa,  $\gamma$ IVa, and  $\gamma$ IV were not as precisely determined as those for the low- $T_c$  proteins,  $\gamma$ II and  $\gamma$ IIIb.

## RESULTS

**Coexistence Curves of Purified  $\gamma$ -Crystallins.** In Fig. 1, we present the coexistence curves for aqueous solutions of calf  $\gamma$ IIIa-,  $\gamma$ IIIb-, and  $\gamma$ IVa-crystallin. Also included in Fig. 1 is the coexistence curve for calf  $\gamma$ II taken from Thomson *et al.* (6) with the protein concentrations recalculated by using the extinction coefficient from Table 1. The solution conditions in Figs. 1–3 are 100 mM phosphate buffer/ionic strength 240 mM, pH 7.1. We find that each coexistence curve can be fit, for temperatures within 10°C of  $T_c$ , to the function (10, 25)

$$|(C_c - C)/C_c| = A[(T_c - T)/T_c]^\beta, \quad [1]$$

where  $\beta = 0.325$ ,  $C_c$  is the critical protein concentration,  $T_c$  is the critical temperature in K, and  $A$  is a parameter that characterizes the width of the coexistence curve. Table 1 displays the values we find for  $C_c$ ,  $T_c$ , and  $A$  for each coexistence curve. These parameters provide a quantitative basis for comparing the measured coexistence curves. One sees that within experimental error,  $A$  and  $C_c$  are the same for all the proteins. In contrast,  $T_c$  is not the same for all the proteins. As Table 1 reveals, the crystallins divide naturally into two groups: high- $T_c$  proteins ( $\gamma$ IIIa and  $\gamma$ IVa) and low- $T_c$  proteins ( $\gamma$ II and  $\gamma$ IIIb).

The protein concentrations in Fig. 1 are indicated in two ways:  $C$  in mg/ml (lower  $x$  axis) and protein volume fraction,

Table 1. Extinction coefficients and coexistence curve parameters for calf  $\gamma$ -crystallins

Crystallin	$E_{280}^{0.1\%,1\text{cm}}$ *	$T_c$ , °C	$C_c$ , mg/ml	$A$
$\gamma$ II	2.18	$5.2 \pm 0.2^\dagger$	$269 \pm 20^\dagger$	$2.6 \pm 0.1^\dagger$
$\gamma$ IIIb	2.11	$5.2 \pm 0.2$	$276 \pm 14$	$2.6 \pm 0.1$
$\gamma$ IIIa	2.33	$36.3 \pm 0.5$	$309 \pm 22$	$2.6 \pm 0.1$
$\gamma$ IVa	2.25	$39.6 \pm 0.3$	$303 \pm 12$	$2.7 \pm 0.1$
$\gamma$ III	2.19 <sup>‡</sup>	$18.5 \pm 0.5^\S$	$293 \pm 33^\S$	$2.5 \pm 0.1^\S$
$\gamma$ IV	2.16	$37.8 \pm 0.6$	$316 \pm 30$	$2.5 \pm 0.1$

\*Extinction coefficients were determined gravimetrically by Pande (A. Pande, personal communication).

<sup>†</sup>Parameters were deduced from a fit to a calibrated coexistence curve from ref. 6.

<sup>‡</sup>Estimated extinction was based on weighted average of extinctions for  $\gamma$ IIIa- and  $\gamma$ IIIb-crystallins.

<sup>§</sup>Parameters were deduced from a fit to a calibrated coexistence curve from ref. 5.

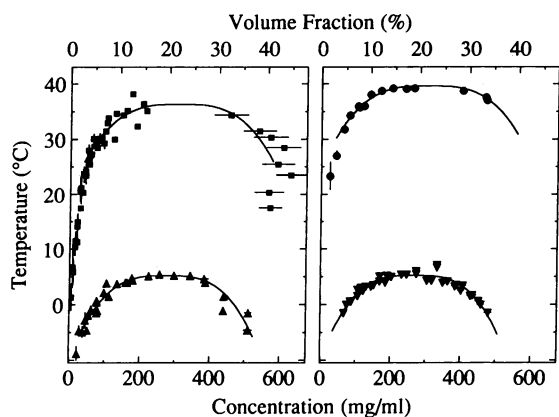


FIG. 1. Coexistence curves for aqueous solutions of purified calf  $\gamma$ -crystallins measured at pH 7.1 in 100 mM phosphate buffer/ionic strength 240 mM. (Left)  $\blacksquare$ ,  $\gamma$ IIIa-crystallin;  $\blacktriangle$ ,  $\gamma$ IIIb-crystallin. (Right)  $\bullet$ ,  $\gamma$ IVa-crystallin;  $\blacktriangledown$ ,  $\gamma$ II-crystallin. ( $\gamma$ II-Crystallin data were taken from ref. 6 with protein concentrations recalculated.) Eq. 1 is fit to each coexistence curve (solid lines).

$\phi$  (upper  $x$  axis). The two sets of units are related by the expression  $\phi = \bar{v} C$ , where  $\bar{v}$  is the partial specific volume of the protein (20). For  $\gamma$ II,  $\bar{v} = (7.1 \pm 0.1) \times 10^{-4} \text{ cm}^3/\text{mg}$  (26); we assume that the partial specific volume is approximately the same for the other  $\gamma$ -crystallins. The coexistence curves in Fig. 1 are determined for protein volume fractions up to  $\approx 40\%$ . The protein volume fractions within crystals of the purified proteins are given in refs. 27 and 28:  $\phi_{\text{xtal}}(\gamma\text{II}) = 57\%$ ,  $\phi_{\text{xtal}}(\gamma\text{IIIb}) = 39\%$ , and  $\phi_{\text{xtal}}(\gamma\text{IVa}) = 62\%$ . For  $\gamma$ IIIb, we obtained protein concentrations in the liquid state nearly equal to the protein concentration in the crystal state.

The experimental uncertainty in the coexistence curves is too large to enable us to determine  $\beta$  precisely. We have chosen to use  $\beta = 0.325$ , the Ising exponent, in Eq. 1 to be consistent with the recent work of Schurtenberger *et al.* (26). They found that Ising, not mean-field exponents, accurately describe the divergence of the intensity of light scattered from aqueous solutions of  $\gamma$ II near the critical point, in accord with the behavior of simple binary mixtures (11). For comparison, we fitted Eq. 1 to our data with  $\beta = 0.5$ , the mean-field exponent. We found that the fits using  $\beta = 0.325$  were clearly better than those using  $\beta = 0.5$ .

Our data indicate that  $C_c$  and  $A$  are approximately the same for the four purified calf  $\gamma$ -crystallin solutions studied (Table 1). The average values of  $C_c$  and  $A$  for  $\gamma$ II,  $\gamma$ IIIa,  $\gamma$ IIIb, and  $\gamma$ IVa are  $C_c = 289 \pm 20 \text{ mg/ml}$  and  $A = 2.6 \pm 0.1$ . This value of  $C_c$  corresponds to a protein volume fraction of  $\phi_c = (20.5 \pm 1.7)\%$ . The fact that  $A$  and  $C_c$  are approximately the same for all the pure  $\gamma$ -crystallin solutions suggests that the underlying free energies for these solutions have a similar functional form.

For lysozyme, another phase-separating globular protein,  $\phi_c = (15.4 \pm 0.7)\%$ , based on published data (22, 29) and a newly determined value for the extinction coefficient of lysozyme  $E_{280}^{0.1\%, 1\text{cm}} = 2.77$  (A. Pande, personal communication). A simple Gibbs free energy model (22) for the behavior of an interacting protein solution predicts that  $\phi_c = 13\%$ .

It is interesting to compare the width  $A$  of  $\gamma$ -crystallin coexistence curves to the width of coexistence curves from other experimental systems. For the liquid-gas phase transition, Guggenheim (30) finds that  $A = 1.75$  for a variety of fluids; the average value of  $A$  for calf  $\gamma$ -crystallins is  $A = 2.6 \pm 0.1$ . For simple binary mixtures, Beysens (11) has fit coexistence curves to the function  $|\phi_c - \phi| = B[(T_c - T)/T_c]^{0.325}$ , where  $\phi$  is the volume fraction of one of the components, and  $\phi_c$  is the critical volume fraction. For a variety of mixtures, he finds that  $B = 0.75\text{--}1.07$ . Our param-

eter  $A$  is related to  $B$  by the expression,  $B = A\phi_c$ . Taking  $\phi_c = 0.205 \pm 0.017$  and  $A = 2.6 \pm 0.1$ , we find that  $B = 0.53 \pm 0.06$  for the  $\gamma$ -crystallins.

**Light Microscopy of Phase Separation.** To supplement our cloud-point and temperature-quench measurements, we studied phase separation by using light microscopy. Crystallin solutions of known concentration, with a sample thickness of  $\approx 100 \mu\text{m}$ , were placed on a thermostated stage, and the temperature of the stage was then lowered 4–6°C below the phase-separation temperature of the sample. The morphology of the protein-poor and protein-rich domains that subsequently formed depended on the concentration of the sample.

In samples with  $C < C_c$ , we observed nucleation and growth of spherical, uniformly sized droplets (Fig. 2a). These droplets contain the protein-rich phase; they are surrounded by the protein-poor phase. While still small in size,  $\approx 1\text{--}5 \mu\text{m}$  in diameter, these droplets undergo noticeable Brownian motion. Touching droplets coalesce, but they do so very slowly on a time scale of several minutes to hours. In samples with  $C > C_c$ , we observed nucleation and growth of uniformly sized droplets once again, but in this case the droplets consist of the protein-poor phase, and the surrounding liquid is the protein-rich phase (Fig. 2c). The high viscosity of the protein-rich phase prevents these droplets from moving or coalescing. In samples with  $C \approx C_c$ , two interconnected domains appear (Fig. 2b). The typical length scale of this bicontinuous network increases slowly in time.

The above observations confirm that over a wide range of protein concentration the reversible clouding that we observe in bulk solutions is caused by binary-liquid phase separation and not by protein crystal formation (24).

Recently, Lo (31) used optical and electron microscopy to study cold cataract in the rat lens. He found that cold-induced opacification of the lens was due to the formation of protein-rich spherical droplets 1.5–10  $\mu\text{m}$  in diameter. The droplets observed by Lo are similar in size, shape, and number density to the droplets that we observe in phase-separated samples of pure  $\gamma$ -crystallin solutions with  $C < C_c$  (Fig. 2a).

We believe that the slow time scale for phase separation in a protein solution makes it an ideal system for studying the kinetics of nucleation and growth (32) and spinodal decomposition (33).

**Coexistence Curves of  $\gamma$ -Crystallin Mixtures.** In Fig. 3, we plot the coexistence curve for calf  $\gamma$ IV-crystallin, the native protein mixture consisting of (by fraction number)  $\approx 85\%$   $\gamma$ IVa and  $\approx 15\%$   $\gamma$ IVb. The ascending limb of the coexistence curve reported by Siezen *et al.* (5) is included in Fig. 3 for comparison. In plotting the data from Siezen *et al.*, we

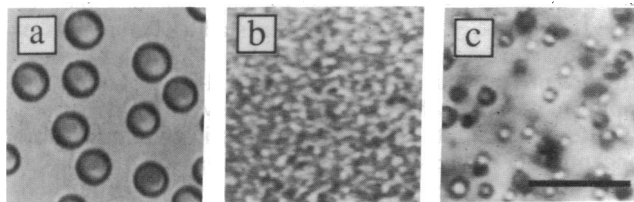


FIG. 2. Optical micrographs of phase separation of calf  $\gamma$ IVa-crystallin solutions for three different protein concentrations quenched  $\Delta T$  below the coexistence curve. The buffer conditions are the same as for Fig. 1. Photographs were taken a few minutes after the temperature was lowered. Similar patterns were seen for other  $\gamma$ -crystallin solutions. (a) Droplets of protein-rich phase surrounded by protein-poor phase ( $C \approx 50 \text{ mg/ml}$ ,  $\Delta T = 6^\circ\text{C}$ ). (b) Bicontinuous entanglement of protein-rich and protein-poor phases ( $C \approx 270 \text{ mg/ml}$ ,  $\Delta T = 6^\circ\text{C}$ ). (c) Droplets of protein-poor phase surrounded by protein-rich phase ( $C \approx 480 \text{ mg/ml}$ ,  $\Delta T = 4^\circ\text{C}$ ). Dark regions represent droplets that are out of focus. (Scale bar =  $20 \mu\text{m}$ ; sample thickness is  $\approx 100 \mu\text{m}$ .)

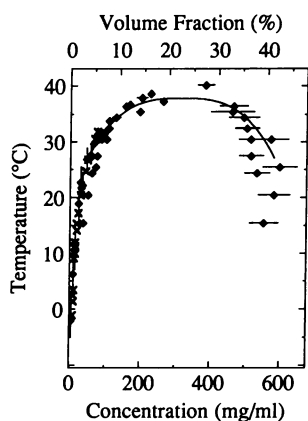


FIG. 3. Coexistence curves for calf  $\gamma$ IV-crystallin ( $\blacklozenge$ ), a native mixture of  $\gamma$ IVa- and  $\gamma$ IVb-crystallin; buffer conditions were the same as for Fig. 1. Included for comparison are the data from ref. 5 ( $\times$ ), which have been calibrated to conform to our experimental conditions; the two data sets agree in the range of overlap. Solid line is the fit of Eq. 1 to our data ( $\blacklozenge$ ) alone.

recalculated the protein concentrations by using the extinction coefficient from Table 1 and subtracted 4°C from their cloud-point temperatures to correct for the fact that they used 50 mM phosphate buffer instead of 100 mM. (We find that  $T_c$  decreases approximately linearly as a function of increasing phosphate buffer concentration in the range 0–100 mM; the slope of this decrease is  $\Delta T_c/\Delta[\text{buffer}] \approx -0.08^\circ\text{C}/\text{mM}$ .) With the above corrections, the data from Siezen *et al.* (5) agrees with ours to within experimental error.

We fitted Eq. 1 to our  $\gamma$ IV coexistence curve data, and the deduced parameters are included in Table 1. The values of  $A$  and  $C_c$  for  $\gamma$ IV-crystallin agree with those for the single-component crystallin solutions. We find that the  $T_c$  for  $\gamma$ IV is 1.8°C below the  $T_c$  for  $\gamma$ IVa, the majority component of  $\gamma$ IV-crystallin.

Siezen *et al.* (5) determined the coexistence curve for calf  $\gamma$ III-crystallin, the native protein mixture consisting of (by fraction number)  $\approx 40\%$   $\gamma$ IIIa and  $\approx 60\%$   $\gamma$ IIIb. We corrected their measured curve, as explained above, and then fitted Eq. 1 to the corrected data. We find that  $T_c = 18.5 \pm 0.5^\circ\text{C}$  for  $\gamma$ III-crystallin; see Table 1. Thus, the critical temperature for  $\gamma$ III falls between the critical temperatures for  $\gamma$ IIIa and  $\gamma$ IIIb.

## DISCUSSION

We have established that purified calf  $\gamma$ -crystallins divide into two distinct groups based on their  $T_c$  values: The low- $T_c$  crystallins,  $\gamma$ II and  $\gamma$ IIIb, with  $T_c \approx 5^\circ\text{C}$ ; and the high- $T_c$  crystallins,  $\gamma$ IIIa and  $\gamma$ IVa, with  $T_c \approx 38^\circ\text{C}$ . The intermediate value of  $T_c$  previously found (5) for calf  $\gamma$ III-crystallin,  $T_c \approx 19^\circ\text{C}$ , is due to the fact that this protein fraction is a mixture of a low- and a high- $T_c$  crystallin. Siezen *et al.* found that the rat (7) and human (8)  $\gamma$ -crystallins also divide into high- and low- $T_c$  groups. Rat  $\gamma$ 2-2,  $\gamma$ 3-1,  $\gamma$ 4-1 and human  $\gamma$ G4 are high- $T_c$  crystallins, and rat  $\gamma$ 1-1,  $\gamma$ 1-2, and  $\gamma$ 2-1 and human  $\gamma$ G3 are low- $T_c$  crystallins.

The amino acid sequences for the calf, rat, and human  $\gamma$ -crystallins are very similar. An examination of sequence homologies indicates that these proteins can be arranged into six orthologous groups  $\gamma$ A– $\gamma$ F (27, 28, 34–36; Table 2). With the crystallins so arranged, one observes a striking correlation: The proteins within each orthologous group exhibit the same phase behavior. For example,  $\gamma$ D-crystallin for all three species is a high- $T_c$  protein. Based on the known  $T_c$  values listed in Table 2, we propose the hypothesis that the proteins in group  $\gamma$ A– $\gamma$ C are necessarily low- $T_c$  proteins, and the proteins in group  $\gamma$ D– $\gamma$ F are necessarily high- $T_c$  proteins.

Table 2. Arrangement of calf, rat, and human  $\gamma$ -crystallins into six orthologous groups  $\gamma$ A– $\gamma$ F

Group name	Calf	Rat	Human
$\gamma$ A	IVb	1-1 (low $T_c$ )	G5 (low $T_c$ )
$\gamma$ B	II (low $T_c$ )	1-2 (low $T_c$ )	1-2
$\gamma$ C	IIIb (low $T_c$ )	2-1 (low $T_c$ )	G3*
$\gamma$ D	IIIa (high $T_c$ )	2-2 (high $T_c$ )	G4 (high $T_c$ )
$\gamma$ E	IVa (high $T_c$ )	3-1 (high $T_c$ )	$\psi$ G2
$\gamma$ F		4-1 (high $T_c$ )	$\psi$ G1

In parentheses we indicate high- $T_c$  and low- $T_c$  crystallins; absence of parentheses implies phase-separation behavior is not known.

\*This  $\gamma$ -crystallin is also designated 2-1.

Under this hypothesis, we predict that calf  $\gamma$ IVb-crystallin is a low- $T_c$  protein.

White *et al.* (27) have shown that the secondary and tertiary structures of calf  $\gamma$ II-crystallin, a low- $T_c$  protein, and calf  $\gamma$ IVa-crystallin, a high- $T_c$  protein, are not significantly different. This finding suggests that the difference in  $T_c$  between group  $\gamma$ A– $\gamma$ C and group  $\gamma$ D– $\gamma$ F proteins may be the result of a few key amino acid residues. A comparison of the known sequences for calf (27, 35, 37, 38), rat (39), and human (40, 41)  $\gamma$ -crystallins, a comparison involving 16 proteins, reveals that the two groups of proteins are differentiated by the identity of the residues at positions 22, 47, and 163. For group  $\gamma$ A– $\gamma$ C, the low- $T_c$  proteins, the residues are Cys-22, Arg-47, and Lys-163. For group  $\gamma$ D– $\gamma$ F, the high- $T_c$  proteins, the residues are His-22, Gln-47, and Arg-163.

The substitution Arg-47  $\rightarrow$  Gln is noteworthy because glutamine is an uncharged residue and arginine is fully ionized (positively charged) at pH 7. The substitution Cys-22  $\rightarrow$  His involves a slight change in charge. At pH 7, cysteine is  $\approx 0.3\%$  negatively charged (assuming  $\text{pK}_a \approx 8-9$ ), and histidine is  $\approx 10\%$  positively charged (assuming  $\text{pK}_a \approx 6-7$ ). The substitution Cys  $\rightarrow$  His is intriguing because it rarely occurs in closely related proteins (42). In contrast, Lys-163  $\rightarrow$  Arg is a charge-conserving substitution. Comparing the sequences of calf  $\gamma$ II- and  $\gamma$ IIIb-crystallins, two proteins with the same  $T_c$ , we find that arginine is replaced by lysine at position 99. This substitution suggests that the Lys-163  $\rightarrow$  Arg substitution does not influence  $T_c$ .

Position 15 may also be important in setting  $T_c$ . For calf and rat  $\gamma$ -crystallins, residue 15 is cysteine for group  $\gamma$ A– $\gamma$ C and histidine for group  $\gamma$ D– $\gamma$ F; this is the same substitution that occurs at position 22. In human  $\gamma$ -crystallin, residue 15 is still histidine for  $\gamma$ D– $\gamma$ F and cysteine for  $\gamma$ A. However, for human  $\gamma$ B and  $\gamma$ C, residue 15 is serine, not cysteine.

The residues at positions 15, 22, 47, and 163 are located on the surface of the proteins, based on the tertiary structure of calf  $\gamma$ II-crystallin (43), which is representative of the structure of all  $\gamma$ -crystallins (27). As a consequence, changes in identity of these residues could significantly change the solvation energy of the protein, which, in turn, could change  $T_c$ .

It is important to note that White *et al.* (27) and Sergeev *et al.* (28) have previously analyzed, in detail, differences in the amino acid sequences of the various  $\gamma$ -crystallins. They sought to relate sequence differences to differences in protein secondary and tertiary structures (27) and to differences in points of contact between lens proteins in the crystal state (27, 28).

**Summary and Conclusion.** We have experimentally measured and quantitatively characterized the coexistence curves for aqueous solutions of several purified calf  $\gamma$ -crystallin lens proteins. We find that the critical concentration  $C_c$  and the width  $A$  of each coexistence curve are, within experimental error, the same for each protein solution studied. In contrast, the critical temperature  $T_c$  for phase separation divides these highly homologous proteins into two distinct groups. One group, consisting of  $\gamma$ II- and  $\gamma$ IIIb-

crystallin, have low phase-separation temperatures:  $T_c \approx 5.2^\circ\text{C}$ . The other group, consisting of  $\gamma\text{IIIa}$ - and  $\gamma\text{IVa}$ -crystallin, have high phase-separation temperatures:  $T_c = 36.3^\circ\text{C}$  for  $\gamma\text{IIIa}$ , and  $T_c = 39.6^\circ\text{C}$  for  $\gamma\text{IVa}$ .

A comparison of the amino acid sequences of calf, rat, and human  $\gamma$ -crystallin suggests that a few key surface residues separate the proteins into high- $T_c$  and low- $T_c$  groups. We propose that the identity of the residues at positions 22, 47, possibly 15, and less likely 163 determines the difference in the  $T_c$  values between the high- $T_c$  and low- $T_c$  proteins. One could test this hypothesis by performing site-directed mutagenesis on the above residues and then measuring  $T_c$  for solutions of the altered protein. Such systematic mutagenesis experiments would also reveal the relative importance of each proposed residue in setting  $T_c$ .

Identification of the above amino acid residues has a potential application for inhibiting cataracts. It has been established in a variety of cataract model systems (13–16) that lens opacification occurs when the phase-separation temperature of the proteins in the lens exceeds body temperature. Such phase-separation cataracts could be suppressed by chemically modifying (44) the lens proteins, so as to decrease  $T_c$  below body temperature. Our results on native calf  $\gamma$ -crystallins identify target sites on these proteins where chemical modifications are likely to produce significant changes in  $T_c$ .

We are grateful to Ajay Pande for measuring the values of the extinction coefficients used in this study and for disclosing his procedure for separating calf  $\gamma\text{IV}$ -crystallin into  $\gamma\text{IVa}$ - and  $\gamma\text{IVb}$ -crystallins before publication. We thank James Melhuish for his technical assistance and Peter Schurtenberger and George Thurston for sharing their insights with us. We also thank Christine Slingsby, Nicolette Lubsen, and Graeme Wistow for providing critical and thoughtful comments on our manuscript. Carolyn Berland gratefully acknowledges support from the National Science Foundation Graduate Fellowship program. This work was supported by grants from the National Eye Institute of the National Institutes of Health (R01 EY05127) and the National Science Foundation (DMR 87-19217).

1. Maisel, H., ed. (1985) *The Ocular Lens* (Marcel Dekker, New York).
2. Wistow, G. J. & Piatigorsky, J. (1988) *Annu. Rev. Biochem.* **57**, 479–504.
3. Nugent, J. & Whelan, J., eds. (1984) *Human Cataract Formation, CIBA Foundation Symposium 106* (Pitman, London).
4. Bloemendal, H., ed. (1981) *Molecular and Cellular Biology of the Eye Lens* (Wiley, New York).
5. Siezen, R. J., Fisch, M. R., Slingsby, C. & Benedek, G. B. (1985) *Proc. Natl. Acad. Sci. USA* **82**, 1701–1705.
6. Thomson, J. A., Schurtenberger, P., Thurston, G. M. & Benedek, G. B. (1987) *Proc. Natl. Acad. Sci. USA* **84**, 7079–7083.
7. Siezen, R. J., Wu, E., Kaplan, E. D., Thompson, J. A. & Benedek, G. B. (1988) *J. Mol. Biol.* **199**, 475–490.
8. Siezen, R. J., Thomson, J. A., Kaplan, E. D. & Benedek, G. B. (1987) *Proc. Natl. Acad. Sci. USA* **84**, 6088–6092.
9. Rowlinson, J. S. & Swinton, F. L. (1982) *Liquids and Liquid Mixtures* (Butterworth, London), 3rd Ed.
10. Heller, P. (1967) *Rep. Prog. Phys.* **30**, 731–826.
11. Beysens, D. (1982) in *Phase Transitions, Cargese 1980*, eds. Levy, M., Le Guillou, J.-C. & Zinn-Justin, J. (Plenum, New York), pp. 25–62.
12. Bungenberg de Jong, H. G. (1949) in *Colloid Science*, ed. Kruyt, H. R. (Elsevier, Amsterdam), Vol. 2, pp. 232–258.
13. Clark, J. I., Giblin, F. J., Reddy, V. N. & Benedek, G. B. (1982) *Invest. Ophthalmol. Visual Sci.* **22**, 186–190.
14. Clark, J. I. & Carper, D. (1987) *Proc. Natl. Acad. Sci. USA* **84**, 122–125.
15. Ishimoto, C., Goalwin, P. W., Sun, S.-T., Nishio, I. & Tanaka, T. (1979) *Proc. Natl. Acad. Sci. USA* **76**, 4414–4419.
16. Tanaka, T., Rubin, S., Sun, S.-T., Nishio, I., Tung, W. & Chylack, L. T. (1983) *Invest. Ophthalmol. Visual Sci.* **24**, 522–525.
17. Björk, I. (1964) *Exp. Eye Res.* **3**, 254–261.
18. Slingsby, C. & Miller, L. R. (1983) *Exp. Eye Res.* **37**, 517–530.
19. Siezen, R. J., Kaplan, E. D. & Anello, R. D. (1985) *Biochem. Biophys. Res. Commun.* **127**, 153–160.
20. van Holde, K. E. (1985) *Physical Biochemistry* (Prentice-Hall, Englewood Cliffs, NJ), 2nd Ed.
21. McDermott, M. J., Gawinowicz-Kolks, M. A., Chiesa, R. & Spector, A. (1988) *Arch. Biochem. Biophys.* **262**, 609–619.
22. Taratuta, V. G., Holschbach, A., Thurston, G. T., Blank-schein, D. & Benedek, G. B. (1990) *J. Phys. Chem.* **94**, 2140–2144.
23. Ishimoto, C. & Tanaka, T. (1977) *Phys. Rev. Lett.* **39**, 474–477.
24. Phillis, G. D. J. (1985) *Phys. Rev. Lett.* **55**, 1341.
25. Stanley, H. E. (1971) *Introduction to Phase Transitions and Critical Phenomena* (Oxford, New York).
26. Schurtenberger, P., Chamberlin, R. A., Thurston, G. M., Thomson, J. A. & Benedek, G. B. (1989) *Phys. Rev. Lett.* **63**, 2064–2067.
27. White, H. E., Driessen, H. P. C., Slingsby, C., Moss, D. S. & Lindley, P. F. (1989) *J. Mol. Biol.* **207**, 217–235.
28. Sergeev, M. V., Chirgadze, Y. N., Mylvaganam, S. E., Driessen, H., Slingsby, C. & Blundell, J. T. (1988) *Proteins* **4**, 137–147.
29. Sophianopoulos, A. J., Rhodes, C. K., Holcomb, D. N. & van Holde, K. E. (1962) *J. Biol. Chem.* **237**, 1107–1112.
30. Guggenheim, E. A. (1967) *Thermodynamics* (North-Holland, New York).
31. Lo, W.-K. (1989) *Proc. Natl. Acad. Sci. USA* **86**, 9926–9930.
32. Cumming, A., Wiltzius, P. & Bates, F. S. (1990) *Phys. Rev. Lett.* **65**, 863–866.
33. Guenoun, P., Gastaud, R., Perrot, F. & Beysens, D. (1987) *Phys. Rev. A* **36**, 4876–4890.
34. Aarts, H. J. M., den Dunnen, J. T., Leunissen, J., Lubsen, N. H. & Schoenmakers, J. G. G. (1988) *J. Mol. Evol.* **27**, 163–172.
35. Hay, R. E., Wood, W. D., Church, R. L. & Petrash, J. M. (1987) *Biochem. Biophys. Res. Commun.* **146**, 332–338.
36. Summers, L. J., Slingsby, C., Blundell, J. T., den Dunnen, J. T., Moormann, R. J. M. & Schoenmakers, J. G. G. (1986) *Exp. Eye Res.* **43**, 77–92.
37. Bhat, S. P. & Spector, A. (1984) *DNA* **3**, 287–295.
38. Chirgadze, Y. N., Nevskaya, N. A., Sergeev, Y. V. & Fomenkova, N. P. (1987) *Mol. Biol. (Moscow)* **21**, 368–376.
39. den Dunnen, J. T., Moormann, R. J. M., Lubsen, N. H. & Schoenmakers, J. G. G. (1986) *J. Mol. Biol.* **189**, 37–46.
40. Meakin, S. O., Breitman, M. L. & Tsui, L.-C. (1985) *Mol. Cell. Biol.* **5**, 1408–1414.
41. Meakin, S. O., Du, R. P., Tsui, L.-C. & Breitman, M. L. (1987) *Mol. Cell. Biol.* **7**, 2671–2679.
42. Creighton, T. E. (1984) *Proteins* (Freeman, New York).
43. Wistow, G., Turnell, B., Summers, L., Slingsby, C., Moss, D., Miller, L., Lindley, P. & Blundell, T. (1983) *J. Mol. Biol.* **170**, 175–202.
44. Pande, J., Berland, C. R., Broide, M. L., Ogun, O. O., Melhuish, J. & Benedek, G. B. (1991) *Proc. Natl. Acad. Sci. USA* **88**, 4916–4920.